Pergamon

Int. J. Heat Mass Transfer. Vol. 37, No. 18, pp. 2901–2908, 1994

0017–9310/94 $7.00+0.00

0017–9310(94)00126–X

Convective instability in a horizontal porous layer saturated with a chemically reacting fluid

M. S. MALASHETTY,† P. CHENG‡ and B. H. CHAO
Department of Mechanical Engineering, University of Hawaii, Honolulu, HI 96822, U.S.A.

(*Received* 8 *July* 1993 *and in final form* 4 *April* 1994)

Abstract—A linear stability analysis has been performed to study the onset of convective instability in a horizontal inert porous layer saturated with a fluid undergoing zero-order exothermic chemical reactions. The horizontal porous layer is cooled from the upper boundary while two different thermal boundary conditions are imposed at the lower boundary, i.e. an isothermal wall and an adiabatic wall. The resulting eigenvalue problems were solved approximately using a single-term Galerkin method that gives the critical Rayleigh number and the associate wave number at a given Frank-Kamenetskii number. It is found that, with chemical reactions, the fluid in the porous medium is more prone to instability as compared to the case in which chemical reactions are absent.

INTRODUCTION

During the past three decades, a great deal of effort has been devoted to the study of free convection in a fluid-saturated porous medium with and without a uniformly distributed heat source with applications to nuclear reactor safety and geothermal reservoir engineering. The studies of onset of free convection and its associate convective pattern in a variety of geometries in these systems have been well documented in the literature [1–3]. However, very little work has been performed on the effect of chemical reactions on free convection in porous media until recently. The increasing interest in this topic has been motivated by its applications to tubular reactors, oxidation of solid materials and synthesis of ceramic materials.

When an exothermic reaction takes place in a fluid-saturated porous medium, the heat generated by the reaction changes the fluid density and free convection may occur. Kordylewski and Krajewski [4] were among the first to consider the interaction of chemical reactions and free convection in a porous medium. They formulated the problem based on Darcy's law with the Boussinesq approximation, assuming that a zero-order exothermic reaction occurs in the fluid phase and that local thermal equilibrium exists between the fluid and the solid phases. The effect of the Rayleigh number on the critical conditions of thermal ignition was investigated. Using the same formulation, Hlavacek and co-workers [5–7] have carried out a numerical solution and a stability analysis on free convection in a confined porous medium with zero-order exothermic reactions. A stability analysis based on the same formulation was recently performed by Farr *et al.* [8]. In a recent paper, Vafai *et al.* [9] obtained a numerical solution for chemically driven convection in a porous cavity with isothermal walls at the top and bottom surfaces and thermally insulated on the side walls; both the inertia and the viscous force are taken into consideration in the momentum equation.

In this paper, we shall study the effect of chemical reaction on the onset of free convection in a horizontal inert porous layer cooled from the upper boundary with two different lower thermal boundary conditions: (1) an isothermal wall; and (2) an adiabatic wall. The assumptions used in the formulation of the problem are the same as those used in the previous work [4–8]. Closed-form solutions for temperature distribution of the two basic undisturbed states corresponding to the two thermal boundary conditions are first obtained; their ignition conditions are thoroughly investigated. A linear stability analysis is then performed and the resulting eigenvalue problems are solved approximately, based on the one-term Galerkin method [10]. The critical Rayleigh number and its associate wave number are obtained for a given value of the Frank-Kamenetskii number. It is found that chemical reactions give rise to nonlinear temperature distributions in the basic undisturbed state that destabilize the fluid in the porous medium. The problem is particularly relevant to the safe operation of an exothermic reactor during its shut-down period [11].

FORMULATION OF THE PROBLEM

Consider a horizontal constant porosity layer of finite thickness, bounded between $z = 0$ and $z = H$ (with z-axis directed vertically upward) and of infinite extent in the horizontal plane (x, y). The inert porous

---

† Fulbright Scholar, on leave from the Department of Mathematics, Gulbarga University, India.

‡ Author to whom correspondence should be addressed.

NOMENCLATURE

a	horizontal wave number
a, b	reaction orders
B	pre-exponential factor
C	constant defined in equation (9)
c_1, c_2	integration constants in equation (17)
D	differentiation with respect to z
E	activation energy
FK	Frank-Kamenetskii number, $QBY_{\mathrm{F}}^{\mathrm{a}}Y_{\mathrm{O}}^{\mathrm{b}}H^2(E/\mathrm{R}T_{\mathrm{c}}^2)\,\mathrm{e}^{-E/\mathrm{R}T_{\mathrm{c}}^2}/\alpha_{\mathrm{m}}$
g	gravitational acceleration
H	thickness of the porous layer
K	permeability
l, m	wave numbers in the x- and y-directions
p	pressure
q	Darcy velocity vector
Q	heat of reaction
R	universal gas constant
Ra	media Rayleigh number for a reacting gas, $g\beta K\mathrm{R}T_{\mathrm{c}}^2/\alpha_{\mathrm{m}}\nu E$
T	temperature
t	time
T_{h}, T_{c}	prescribed temperatures of the lower and upper porous layer
T_{r}	a characteristic temperature for a reacting gas, $\mathrm{R}T_{\mathrm{c}}^2/E$
u, v, w	velocity components
W	function defined in equation (36)
x, y, z	coordinates
X, Y	quantities defined in equation (46)
Y_{O}	mass fraction of oxidizer
Y_{F}	mass fraction of fuel.

Greek symbols

α_{m}	effective thermal diffusivity of the saturated porous medium
β	thermal expansion coefficient
θ	dimensionless temperature
Θ	function defined in equation (37)
ν	kinematic viscosity
ρ	density
σ	heat capacity ratio of the saturated porous medium to that of the gas
ω	growth rate.

Subscript

b	basic undisturbed state.

Superscripts

*	dimensionless quantity
′	disturbed quantity.

layer is saturated with a chemically reactive gas subject to weakly exothermic chemical reactions and is cooled from the top at a temperature of T_{c}. If the temperature in the whole domain of interest varies only slightly from T_{c}, a zero-order reaction can be assumed and the Boussinesq approximation can be invoked. Moreover, it is assumed that local thermal equilibrium exists between the solid matrix and the saturated fluid. With these assumptions, the governing equations in a Cartesian coordinate system (x, y, z) for convection in a porous medium, based on Darcy's law, are:

$$\frac{\partial u}{\partial x}+\frac{\partial v}{\partial y}+\frac{\partial w}{\partial z}=0 \tag{1}$$

$$\bar{q}=-\frac{\mu}{K}(\nabla p+\rho\bar{g}) \tag{2}$$

$$\rho=\rho_0[1-\beta(T-T_{\mathrm{c}})] \tag{3}$$

$$\sigma\frac{\partial T}{\partial t}+\bar{q}\cdot\nabla T=\alpha_{\mathrm{m}}\nabla^2T+QBY_{\mathrm{F}}^{\mathrm{a}}Y_{\mathrm{O}}^{\mathrm{b}}\exp\left[-\frac{E}{\mathrm{R}T}\right], \tag{4}$$

where $\bar{q}=\bar{i}u+\bar{j}v+\bar{k}w$ is the Darcy velocity vector, p and T are the pressure and temperature, t is the time, σ is the heat capacity ratio of the saturated porous medium to that of the gas, ρ, μ, and β are the density, viscosity and the thermal expansion coefficient of the gas, K is the permeability, α_{m} is the effective stagnant thermal conductivity of the saturated porous medium, Q is the heat of reaction, B is the pre-exponential factor, E is the activation energy, R is the universal gas constant, Y_{F} and Y_{O} are mass fractions of fuel and oxidizer, and a and b are their respective reaction order. Examing the chemical reaction term in equation (4), we note that there are two possibilities for the existence of zero-order reactions. The first is the case of a = b = 0, which means that the chemical reaction does not depend on the concentrations of reactants. This is obviously unrealistic because this implies that chemical reaction can occur without the presence of reactants. The second case is that only a negligible amount of reactant is depleted during the reaction, which is observable only for the weakly reacted situation in a flow with a small temperature variation, as the problem analyzed in this study. Clearly, for the vigorous combustion case, chemical reaction depends strongly on the concentration of reactants and hence zero-order reaction cannot be applied. Similarly, in a flow field with a moderate temperature variation, the reactant concentrations are functions of position (because the reaction rate is a function of temperature) so that the zero-order reaction cannot be applied either.

The hydrodynamic boundary conditions for this problem are

$$w(x,y,0) = 0, \quad w(x,y,H) = 0 \qquad (5a, b)$$

and the thermal boundary condition at the top of the porous layer is given by

$$T(x,y,H) = T_c. \qquad (6)$$

For the bottom thermal boundary condition, we consider two different cases: an isothermal wall and an adiabatic wall. The thermal boundary conditions corresponding to these two cases are:

case 1—an isothermal wall,

$$T(x,y,0) = T_h, \qquad (7)$$

where $T_h > T_c$;

case 2—an adiabatic wall,

$$\frac{\partial T}{\partial z}(x,y,0) = 0. \qquad (8)$$

We now assume that the fluid in the porous medium is subject to a high-activation energy reaction such that $RT_c/E \ll 1$. With this approximation, equation (4) can be simplified to

$$\sigma\frac{\partial\theta}{\partial t} + \bar{q}\cdot\nabla\theta = \alpha_m\nabla^2\theta + C\exp[\theta], \qquad (9)$$

where $C = QBY_F^a Y_O^b \exp(-E/RT_c)$ and $\theta = (T-T_c)/T_r$ with $T_r = RT_c^2/E$ being the prescribed reference temperature for a reacting gas. Equation (6) in terms of θ reduces to

$$\theta(x,y,1) = 0, \qquad (10)$$

while boundary conditions (7) and (8) become

$$\theta(x,y,0) = \theta_h \qquad (11)$$

$$\frac{\partial\theta}{\partial z}(x,y,0) = 0, \qquad (12)$$

where $\theta_h = (T_h - T_c)/(RT_c^2/E)$.

BASIC UNDISTURBED STATES AND IGNITION CONDITIONS

We now consider the two basic undisturbed states corresponding to the two different thermal boundary conditions at the lower boundary. At an undisturbed state, we have:

$$\bar{q} = (u,v,w) = (0,0,0) \qquad (13a)$$

$$\theta = \theta_b(z), \quad p = p_b(z), \quad \text{and} \quad \rho = \rho_b(z) \qquad (13b\text{–}d)$$

and equations (2) and (4) reduce to:

$$\frac{dp_b}{dz} + \rho_b g = 0 \qquad (14)$$

$$\alpha_m\frac{d^2\theta_b}{dz^2} + Ce^{\theta_b} = 0. \qquad (15)$$

Equation (15) can be rewritten in the dimensionless form as

$$\frac{d^2\theta_b}{dz^*} = -FKe^{\theta_b}, \qquad (16)$$

with $z^* = z/H$ and $FK = C(H^2/\alpha_m)(E/RT_c^2)$ being the so-called Frank-Kamenetskii number which is commonly called the reduced Damköhler number in the combustion literature. Physically, the FK number is a ratio of the characteristic flow time to the characteristic reaction time. Integrating equation (16) yields the following general solution:

$$\theta_b = \ln\left(\frac{c_1}{2FK}\right) + \ln\left[1 - \left(\frac{1 - c_2 e^{-\sqrt{c_2}z^*}}{1 + c_2 e^{-\sqrt{c_2}z^*}}\right)^2\right], \quad \textit{for}\ FK \neq 0, \qquad (17)$$

where c_1 and c_2 are the integration constants to be determined.

For case 1, applying the following isothermal boundary conditions,

$$\theta_b = \theta_h \quad \text{at}\ z^* = 0 \quad \text{and} \quad \theta_b = 0 \quad \text{at}\ z^* = 1 \qquad (18a, b)$$

gives c_1 implicitly by the following equation:

$$e^{\sqrt{c_1}}\left(\frac{1 - \sqrt{1 - \frac{2FK}{c_1}}}{1 + \sqrt{1 - \frac{2FK}{c_1}}}\right) = \left(\frac{1 - \sqrt{1 - \frac{2FK}{c_1}e^{\theta_h}}}{1 + \sqrt{1 - \frac{2FK}{c_1}e^{\theta_h}}}\right) \qquad (19a)$$

and c_2 by

$$c_2 = e^{\sqrt{c_1}}\left(\frac{1 - \sqrt{1 - \frac{2FK}{c_1}}}{1 + \sqrt{1 - \frac{2FK}{c_1}}}\right). \qquad (19b)$$

It follows from equation (19a) that c_1 is a function of FK and θ_h.

For this case, ignition begins when the self-sustainable or adiabatic condition occurs at the lower boundary, i.e.

$$\frac{d\theta}{dz^*}(0) = 0. \qquad (20a)$$

This condition means that the heat generated by the reaction is high enough to support further reaction without the aid of heat transfer from the wall. Applying equation (20a) to equation (19a) gives

$$c_1 = 2FKe^{\theta_h}. \qquad (20b)$$

Substituting the above equation into equation (19b) yields the following critical value of FK at ignition:

$$(FK)_c = \frac{1}{2e^{\theta_h}}\left[\ln\left(\frac{1 - \sqrt{1 - e^{-\theta_h}}}{1 + \sqrt{1 - e^{-\theta_h}}}\right)\right]^2. \qquad (21)$$

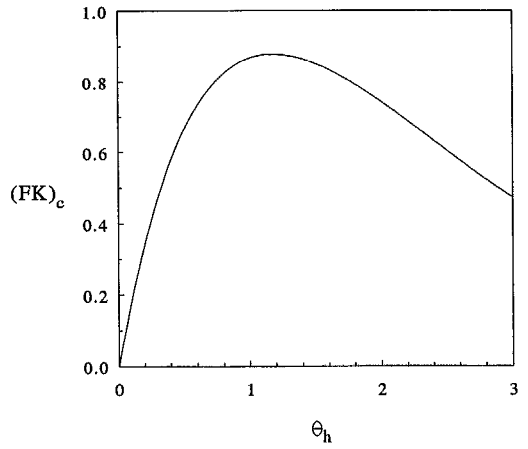

Fig. 1. Effect of wall temperature on the critical value of *FK* for case 1.

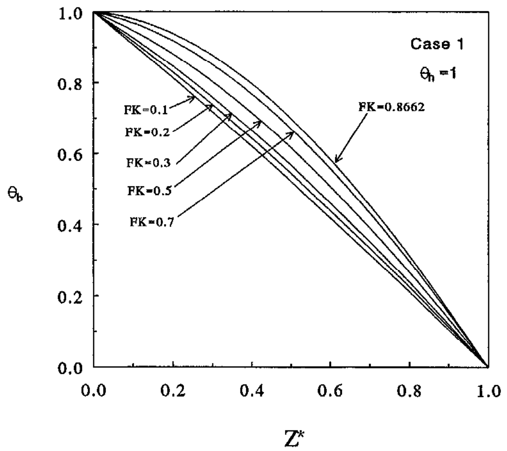

Fig. 2. Basic temperature profiles at different values of *FK* for case 1.

The effect of θ_h on this critical value of *FK* is presented in Fig. 1. It is shown that the critical value of *FK* increases to a maximum value of 0.8785 (corresponding to $\theta_h = 1.19$) and then decreases as θ_h is increased (see also Table 1).

Computations for c_1 and c_2 from equations (19) were carried out for selected values of θ_h and with different values of *FK* up to their ignition values. The results of these computations for $\theta_h = 1$ are listed in Table 2. The corresponding undisturbed temperature profiles are presented in Fig. 2. It is shown that, at small values of *FK*, the basic temperature profile is almost linear with the vertical coordinate z^*. Because chemical reactions give rise to heat generation, the basic undisturbed temperature profile becomes more nonlinear as the value of *FK* is increased for a higher heat generation rate.

Table 1. Critical values of *FK* at different values of θ_h for case 1

θ_h	FK_c
0.50	0.6587
1.00	0.8662
1.08	0.8746
1.19	0.8785
1.20	0.8784
1.22	0.8781
1.50	0.8523
2.00	0.7435
3.00	0.4734

Table 2. Values of c_1, c_2, a_c and Ra_c for case 1 with $\theta_h = 1$

FK	c_1	c_2	a_c	Ra_c
0	—	—	3.141	39.47
0.1	1.351	0.1279	3.109	38.53
0.2	1.718	0.2453	3.082	38.69
0.3	2.102	0.3572	3.059	36.98
0.4	2.505	0.4667	3.040	36.37
0.5	2.930	0.5759	3.024	35.84
0.6	3.378	0.6866	3.012	35.38
0.7	3.852	0.8003	3.003	34.98
0.8	4.357	0.9185	2.996	34.63
0.8662	4.675	0.9924	2.990	33.75

For case 2, the dimensionless thermal boundary conditions are

$$\frac{d\theta_b}{dz^*} = 0 \quad \text{at } z^* = 0 \quad \text{and} \quad \theta_b = 0 \quad \text{at } z^* = 1, \tag{22a, b}$$

which can be applied to determine c_1 and c_2. This gives

$$e^{\sqrt{c_1}}\left(1-\sqrt{1-2FK/c_1}\right) = \left(1+\sqrt{1-2FK/c_1}\right) \tag{23a}$$

$$c_2 = 1. \tag{23b}$$

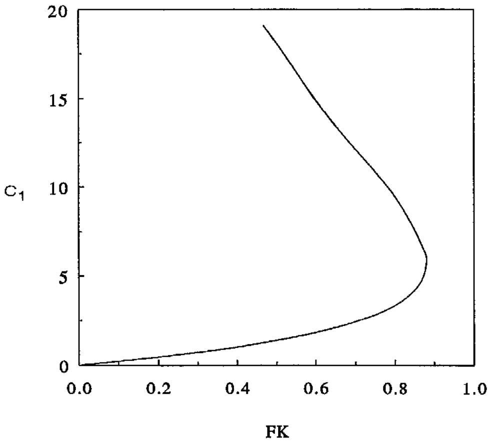

Fig. 3. Values of c_1 vs *FK* for case 2.

The implicit relation between c_1 and *FK* given by equation (23a) is illustrated in Fig. 3, which shows that no solution exists for c_1 beyond a critical value of *FK*. Note that Fig. 3 is just a scaled plot of the typical

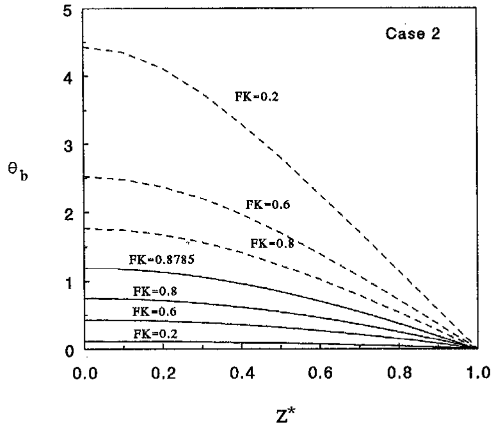

Fig. 4. Basic temperature profiles at different values of *FK* for case 2.

Frank-Kamenetskii's bifurcation diagram [12]. For *FK* less than this critical value, there are two values of c_1 which correspond to two basic undisturbed temperature profiles. The critical value of *FK* beyond which no solution exists for this weakly reactive case is then defined as the ignition state. For values of *FK* higher than this critical value, the solution jumps to the vigorous combustion case (i.e. the upper branch of the S-shaped ignition–extinction curve), which is beyond the scope of this study. It follows that the criteria for ignition is

$$\frac{\partial FK}{\partial c_1} = 0. \tag{24}$$

A differentiation of equation (23a) with respect to c_1 gives

$$c_1 = 2FK + 4. \tag{25}$$

Substituting equation (25) into equation (23a) yields

$$e^{\sqrt{2FK+4}} = \frac{\sqrt{2FK+4}+2}{\sqrt{2FK+4}-2}. \tag{26}$$

A numerical solution of equation (26) gives $FK = 0.8785$, which is the critical value of *FK* at ignition for case 2. This critical value of *FK* was given previously by Frank-Kamenetskii [12]. The two basic undisturbed temperature profiles for case 2 corresponding to two values of c_1 for *FK* at 0.2, 0.6 and 0.8 (i.e. less the critical value of 0.8785) are presented in Fig. 4. The dashed lines (corresponding to the upper branch of c_1) are known to be physically unrealistic in combustion literature, because the temperature increases as the value of *FK* (or heat generation) is decreased. They are referred to as the unstable states in the chemical reactor literature. The solid lines represent the physically realistic cases (corresponding to the lower branch of c_1), where temperature increases as the value of *FK* is increased, as it should. Note that, for physically realistic cases, the temperature profile becomes more nonlinear as the value of *FK* increases (meaning a stronger chemical reaction). The values of c_1 for a physically realistic case at different values of *FK* are listed in Table 3.

The temperature of the adiabatic wall can be obtained from equation (17) to give

$$\theta_b(0) = \theta_h = \ln\left(\frac{c_1}{2FK}\right). \tag{27}$$

Substituting the above equation into equation (23a) yields

$$FK = \frac{1}{2e^{\theta_b}}\left[\ln\left(\frac{1-\sqrt{1-e^{-\theta_b}}}{1+\sqrt{1-e^{-\theta_b}}}\right)\right]^2, \tag{28}$$

which is identical to equation (21) if *FK* in equation (28) is replaced by $(FK)_c$. Thus, equation (28) can also be represented by Fig. 1 if $(FK)_c$ is replaced by *FK*. Under this situation, the maximum value of *FK* (i.e. $FK = 0.8785$) corresponds to the critical value of *FK* for case 2 and the right-hand side of the curve represents the adiabatic wall temperature of the physically unrealistic cases.

LINEAR STABILITY ANALYSIS

We now perform a linear stability analysis by letting

$$\begin{aligned}\bar{q} &= \bar{i}u' + \bar{j}v' + \bar{k}w' \\ p &= p_b(z) + p'(x, y, z, t) \\ \rho &= \rho_b(z) + \rho'(x, y, z, t) \\ \theta &= \theta_b(z) + \theta'(x, y, z, t),\end{aligned} \tag{29}$$

where the primes indicate small perturbations from the undisturbed state. Substituting equation (29) into equations (1)–(3) and (9) and neglecting nonlinear terms, we obtain the following linear equations in terms of w' and θ':

$$\nabla^2 w' = \frac{g\beta K \mathrm{R} T_c^2}{\nu E}\nabla_1^2\theta' \tag{30}$$

$$\sigma\frac{\partial\theta'}{\partial t} + w'\frac{d\theta_b}{dz} = \alpha_m\nabla^2\theta' + Ce^{\theta_b}\theta', \tag{31}$$

where $\nabla_1^2 = (\partial^2/\partial x^2) + (\partial^2/\partial y^2)$. Equations (30) and (31) can be expressed in the following dimensionless form:

$$\nabla^2 w^* = Ra\left(\frac{\partial^2\theta'}{\partial x^{*2}} + \frac{\partial^2\theta'}{\partial y^{*2}}\right) \tag{32}$$

$$\frac{\partial\theta'}{\partial t^*} + w^*\frac{d\theta_b}{dz^*} = \left(\frac{\partial^2\theta'}{\partial x^{*2}} + \frac{\partial^2\theta'}{\partial y^{*2}} + \frac{\partial^2\theta'}{\partial z^{*2}}\right) + FKe^{\theta_b}\theta', \tag{33}$$

where $w^* = w'H/\alpha_m$, $(x^*, y^*, z^*) = (x, y, z)/H$, $t^* = \alpha_m t/\sigma H^2$ and

$$Ra = \frac{g\beta KHT_r}{\nu\alpha_m} = \frac{g\beta KH\mathrm{R}T_c^2}{\nu\alpha_m E}$$

is the media Rayleigh number for a reacting gas in porous media [4].

The boundary conditions in terms of w^* and θ' for the two cases are

$$w^* = 0 \quad \text{at} \quad z^* = 0, 1 \tag{34a}$$

$$\theta' = 0 \quad \text{at} \quad z^* = 0, 1 \tag{34b}$$

and

$$w^* = 0 \quad \text{at} \quad z^* = 0, 1 \tag{35a}$$

$$\theta' = 0 \quad \text{at} \quad z^* = 0 \tag{35b}$$

$$\frac{\partial \theta'}{\partial z^*} = 0 \quad \text{at} \quad z^* = 1. \tag{35c}$$

We now assume that the solution for equations (32) and (33) is in the form

$$w^* = W(z^*) \exp [i(lx + my - \omega t)] \tag{36}$$

and

$$\theta' = \Theta(z^*) \exp [i(lx + my - \omega t)], \tag{37}$$

where l and m are the dimensionless wave numbers in the x- and y-directions. Substituting equations (36) and (37) in equations (32) and (33) gives

$$(\mathrm{D}^2 - a^2) W = -Ra^2 \Theta \tag{38}$$

$$-\omega \Theta + W \frac{\mathrm{d}\theta_\mathrm{b}}{\mathrm{d}z^*} = (\mathrm{D}^2 - a^2)\Theta + FK\mathrm{e}^{\theta_\mathrm{b}}\Theta, \tag{39}$$

where $a = \sqrt{l^2 + m^2}$ is the dimensionless horizontal wave number and $\mathrm{D} = (\mathrm{d}/\mathrm{d}z^*)$. For the marginal stability at which $\omega = 0$, equation (39) becomes

$$(\mathrm{D}^2 - a^2)\Theta - W \frac{\mathrm{d}\theta_\mathrm{b}}{\mathrm{d}z^*} + FK\mathrm{e}^{\theta_\mathrm{b}}\Theta = 0. \tag{40}$$

Equations (38) and (40), subject to the homogeneous boundary conditions (34) or (35), are an eigenvalue problem, with Ra being the eigenvalue.

APPROXIMATE SOLUTIONS FOR THE EIGENVALUE PROBLEMS

An approximate solution for the eigenvalue can be obtained by the Galerkin method [10]. To this end, we let

$$W = A_1 W_1 \quad \text{and} \quad \Theta = B_1 \Theta_1, \tag{41}$$

where W_1 and Θ_1 are the trial functions which must satisfy the boundary conditions (34) or (35). Substituting equation (41) in equations (38) and (40), multiplying the resulting equations by W_1 and by Θ_1, respectively, integrating each equation from $z^* = 0$ to $z^* = 1$ and performing some integration by parts, we obtain

$$A_1[\langle (\mathrm{D}W_1)^2 + a^2 W_1 \rangle] + B_1 a^2 Ra \langle W_1 \Theta_1 \rangle = 0 \tag{42}$$

$$A_1 \left\langle W_1 \Theta_1 \frac{\mathrm{d}\theta_\mathrm{b}}{\mathrm{d}z^*} \right\rangle + B_1[\langle -(\mathrm{D}\Theta_1)^2 - a^2 (\Theta_1)^2 + FK\mathrm{e}^{\theta_\mathrm{b}}\Theta_1^2 \rangle] = 0, \tag{43}$$

where $\langle \mathrm{f} \rangle = \int_0^1 \mathrm{f}\, \mathrm{d}z^*$. Eliminating A_1 and B_1 between equations (42) and (43), we obtain the following equation for the Rayleigh number (Ra):

$$Ra = -\frac{\langle (\mathrm{D}W_1)^2 + a^2 W_1 \rangle \langle (\mathrm{D}\Theta_1)^2 + a^2\Theta_1^2 - FK\mathrm{e}^{\theta_\mathrm{b}}\Theta_1^2 \rangle}{a^2 \langle W_1 \Theta_1 \rangle \left\langle W_1 \Theta_1 \frac{\mathrm{d}\theta_\mathrm{b}}{\mathrm{d}z^*} \right\rangle}. \tag{44}$$

For case 1, we choose the trial functions as

$$W_1(z^*) = \sin \pi z^* \tag{45a}$$

$$\Theta_1(z^*) = \sin \pi z^*, \tag{45b}$$

which satisfy the boundary conditions (34). Substituting equations (45) in equation (44) gives

$$Ra = -(\pi^2 + a^2)(\pi^2 + a^2 - X)/(2a^2 Y), \tag{46}$$

where

$$X = 2FK\langle \mathrm{e}^{\theta_\mathrm{b}}\Theta_1^2 \rangle \quad \text{and} \quad Y = \left\langle W_1 \Theta_1 \frac{\mathrm{d}\theta_\mathrm{b}}{\mathrm{d}z^*} \right\rangle,$$

whose values can be obtained by numerical integration. The minimum value of the Rayleigh number Ra occurs at

$$a_\mathrm{c} = \{\pi \sqrt{(\pi^2 - X)}\}, \tag{47}$$

which is the horizontal wave number at the onset of free convection. Equation (47) is obtained by differentiating equation (46) with respect to a. Substituting equation (47) in equation (46) gives the value of the critical Rayleigh number. Note that, for $FK = 0$ and $\theta_\mathrm{h} = 1$ (and consequently $X = 0$ and $Y = -1/2$), equations (47) and (46) give $a_\mathrm{c} = \pi$ and $Ra_\mathrm{c} = 4\pi^2$, where the Rayleigh number is defined based on the characteristic temperature difference $\Delta T_\mathrm{r} = (T_\mathrm{h} - T_\mathrm{c})$ at which no chemical reactions take place. These values of a_c and Ra_c are exactly the same values obtained previously by Lapwood [13].

The critical Rayleigh number Ra_c as a function of FK at selected values of θ_h for case 1 is presented in Fig. 5. It is shown that the critical Rayleigh number decreases as the value of FK is increased. Thus, chemical reaction in a horizontal porous layer enhances instability. This is reasonable because chemical reaction leads to non-linear temperature distribution in the undisturbed state. The value of the wave number at the onset of convection a_c as a function of FK for this case is presented in Fig. 6 which decreases asymptotically. The variations of the critical Rayleigh number and the wave number as a function of FK are small. The values of Ra_c and a_c for case 1 with $\theta_\mathrm{h} = 1$ are also listed in Table 2.

For case 2, we choose the trial functions as

$$W_1(z^*) = \sin \pi z^* \tag{48a}$$

$$\Theta_1(z^*) = \cos (\pi/2) z^*, \tag{48b}$$

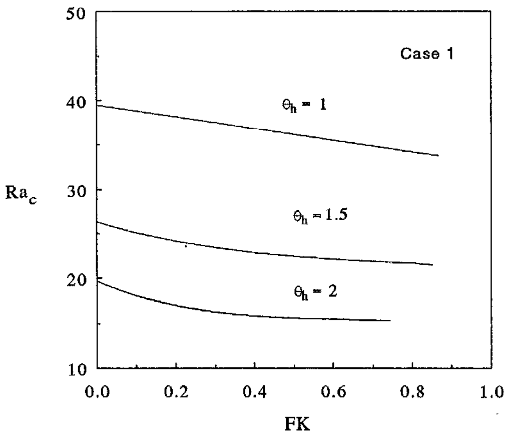

Fig. 5. Critical Rayleigh number vs *FK* for case 1.

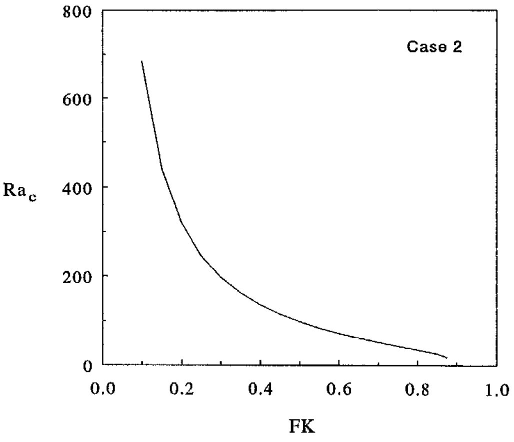

Fig. 7. Critical Rayleigh number vs *FK* for case 2.

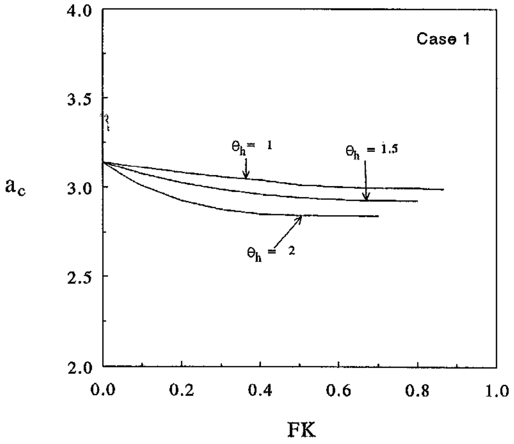

Fig. 6. Critical wave number vs *FK* for case 1.

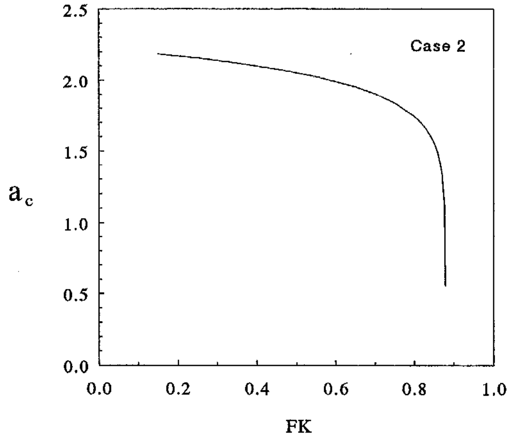

Fig. 8. Critical wave number vs *FK* for case 2.

which satisfy the boundary conditions (35). Substituting these trial functions into equation (44) yields

$$Ra = -\frac{3\pi}{64}\frac{(\pi^2+a^2)(\pi^2+4a^2-4X)}{a^2Y}. \quad (49)$$

The minimum value of the Rayleigh number occurs at

$$a_c = \left[\frac{\pi}{2}\sqrt{\pi^2-4X}\right]. \quad (50)$$

The critical Rayleigh number as a function of *FK* for the physically realistic cases is presented in Fig. 7. It is seen that the critical Rayleigh number decreases drastically from infinity (i.e. unconditionally stable) as the *FK* value increases from zero. The corresponding critical wave number decreases as the value of *FK* is increased, as shown in Fig. 8. The decrease in the critical wave number is drastic near the ignition point. These values of Ra_c and a_c are also listed in Table 3.

Table 3. Values of c_1, a_c and Ra_c for case 2

FK	c_1	a_c	Ra_c
0.1	0:2107	2.198	684.3
0.2	0.4463	2.171	319.7
0.3	0.7135	2.139	197.5
0.4	1.022	2.101	135.7
0.5	1.389	2.054	98.04
0.6	1.843	1.993	72.06

CONCLUDING REMARKS

The effect of zero-order exothermic chemical reaction on the onset of free convection in a fluid-saturated porous medium has been investigated in this paper. The chemical reaction leads to a distributed heat source which gives rise to a nonlinear temperature distribution in the undisturbed state. Thus, the effect of chemical reactions is to enhance the onset of free convection compared to the case in which chemical reactions are absent.

Acknowledgments—One of the authors (M.S.M.) is grateful to the United States Information Agency for the financial support under its Fulbright program and to the University Grants Commission India for travel grants. The senior author (P.C.) wishes to thank Professor D. Vortmeyer of the Technical University of Munich for suggesting the problem for investigation. The authors would like to thank Tim Zhao for his assistance in the preparation of the graphs and an anonymous reviewer for calling our attention to ref. [8], which we were unaware of at the time this work was performed.

REFERENCES

1. R. D. Gasser and M. S. Kazimi, Onset of convection in a porous medium with internal heat generation, *J. Heat Transfer* **98,** 49–54 (1976).
2. P. Cheng, Heat transfer in geothermal systems, *Adv. Heat Transfer* **14,** 1–105 (1978).
3. D. A. Neild and A. Bejan, *Convection in Porous Media.* Springer, New York (1992).
4. W. Kordylewski and Z. Krajewski, Convection effects on thermal ignition in porous media, *Chem. Engng Sci.* **39,** 610–612 (1984).
5. J. E. Gatica, H. J. Viljoen and V. Hlavacek, Thermal instability of nonlinear stratified fluids, *Int. Communs Heat Mass Transfer* **14,** 673–686 (1987).
6. J. E. Gatica, H. Viljoen and V. Hlavacek, Stability analysis of chemical reaction and free convection in porous media, *Int. Communs Heat Mass Transfer* **14,** 391–403 (1987).
7. H. Viljoen and H. Hlavacek, Chemically driven convection in a porous medium, *A.I.Ch.E. Jl* **33,** 1344–1350 (1987).
8. W. W. Farr, J. F. Gabitto, D. Luss and V. Balakotaiah, Reaction-driven convection in a porous medium, *A.I.Ch.E. Jl* **37,** 963–985 (1991).
9. K. Vafai, C. P. Desai and S. C. Chen, An investigation of heat transfer process in a chemically reacting packed bed, *Numer. Heat Transfer* **24,** 127–142 (1993).
10. B. A. Finlayson, *The Method of Weighted Residuals and Variational Principles.* Academic Press, New York (1972).
11. D. Vortmeyer, private communications (1984).
12. D. A. Frank-Kamenetskii, *Diffusion and Heat Exchange in Chemical Kinetics.* Plenum, New York (1969).
13. E. R. Lapwood, Convection of a fluid in a porous medium, *Proc. Camb. Phil. Soc.* **44,** 508–521 (1948).